Contrast Source Inversion of 3D Electromagnetic Data

P. M. van den Berg
Delft University of Technology, The Netherlands

A. Abubakar and T. M. Habashy
Schlumberger-Doll Research, USA

Abstract—This paper discusses the full vector three-dimensional inverse electromagnetic scattering problem. We consider the determination of the location and the electromagnetic composition of an inhomogeneous bounded object in a homogeneous embedding from measurements of the scattered electromagnetic wavefield, when the object is illuminated by a known single frequency wavefield. To solve this large-scale nonlinear inversion problem, we apply the so-called multiplicative regularized contrast source method.

1. Introduction

In this MR-CSI method we reconstruct the complex permittivity contrast and the so-called contrast sources (the product of the contrast and the fields) by minimizing a cost functional in which the residual errors in the field equations occur. This minimization is carried out in an alternating way. In each iterative step we update the contrast and the contrast sources each using one conjugate gradient step so that the total computational complexity of the method is equal to the complexity of solving only two forward problems. By operating in this manner solving a full three-dimensional vector nonlinear inverse scattering problem is feasible. Further this method is equipped with total variation type regularization. This regularization is included as a multiplicative constraint, so that the regularization parameter needed in the minimization process is determined automatically. The multiplicative type of regularization handles noisy as well as limited data in a robust way without the usually necessary a *priori* information. We illustrate the performance by presenting some inversion results from 3D electromagnetic experimental data. Further, we discuss an inversion method to invert not only the complex electric contrast but also the magnetic contrast of a three-dimensional object. The contrast source inversion is extended by introducing both the electric contrast sources and the magnetic contrast sources. Further, an extended cost functional is introduced in which the residual errors in both the electric and magnetic field equations occur. Additionally, the multiplicative regularization is extended such that the spatial variations of both the electric and magnetic contrast are minimized. Since in [1] we tested the algorithm for a heterogeneous object that has intermingled electric and magnetic contrast, we will present a numerical example with disjoint electric and magnetic contrast.

2. Inversion Algorithm

The Multiplicative Regularized Born Inversion (MRCSI) consists of an algorithm to construct sequences $w_j = \{w_{j,n}\}$ and $\chi = \{\chi_n\}$ which iteratively reduce the value of the cost functional,

$$F_n = [F_S + F_{D,n}]F_n^R = \left[\frac{\sum_j \|u_j^{\mathrm{sct}} - G_S w_j\|_S^2}{\sum_j \|u_j^{\mathrm{sct}}\|_S^2} + \frac{\sum_j \|\chi u_j^{\mathrm{inc}} - w_j + G_D w_j\|_D^2}{\sum_j \|\chi_{n-1} u_j^{\mathrm{inc}}\|_D^2}\right] \frac{1}{V} \int_D \frac{|\nabla\chi|^2 + \delta_n^2}{|\nabla\chi_{n-1}|^2 + \delta_n^2} dv$$

where
$[G_S w_j](\bar{x}) = \int_D g(\bar{x}, \bar{x}') w_j(\bar{x}') dv(\bar{x}')$, $\bar{x} \in S$, and $[G_D w_j](\bar{x}) = \int_D g(\bar{x}, \bar{x}') w_j(\bar{x}') dv(\bar{x}')$, $\bar{x} \in D$. The subscripts D and S indicate that the observation point $\bar{x}$ lies either in D, a bounded domain containing the scattering object, or S, a domain disjoint from D on which the scattered field u_j^{sct}, $j = 1, \ldots, J$, is measured for each known incident field u_j^{inc}. The symbol V denotes the volume of the domain D. Further, $\|\bullet\|_S$ and $\|\bullet\|_D$ denote the norms on $L_2(S)$ and $L_2(D)$. Further, g denotes the Green function of the background medium, while χ denotes the contrast with the background medium. For the steering parameter δ_n^2 we choose progressively decreasing values in such a way that, for given contrast sources, the cost functional F_n as a function of the contrast χ, remains convex during all iterations. We relate this parameter directly to the decreasing object error $F_{D;n-1}$. The structure of the cost functional is such that it will minimize the regularization factor F_n^R with a large weighting parameter in the beginning of the optimization process, because the value of $F_S + F_{D;n-1}$ is still large, and that it will gradually minimize more and more the error in the data and object equations when the value of F_n^R has reached a nearly constant value equal to one. If noise is present in the data, the data error term F_S will remain at a large value during the optimization and therefore, the weight of the regularization factor will be more significant. Hence, the hindering character of noise will, at all times, be suppressed in the reconstruction

process, but at the cost of decreased resolution. This minimization is carried out in two alternate steps. For given contrast, χ_{n-1}, the contrast sources are updated via conjugate gradient directions of the cost functional, while for given contrast sources, $w_{j,n}$, the contrast is updated via a preconditioned conjugate gradient direction of the cost functional.

3. Integral Operators for Electric Contrast

Firstly we consider the 3D electromagnetic inversion problem, where the scattering object only has electric contrast χ^E with respect to its embedding. Then we deal with electric contrast sources

$$\bar{w}_j^E(\bar{x}) = \chi^E(\bar{x})\bar{E}(\bar{x}), \quad \text{where} \quad \chi^E(\bar{x}) = \frac{\sigma'(\bar{x})}{\sigma'_b} - 1,$$

with complex conductivity, $\sigma'(\bar{x}) = \sigma(\bar{x}) - i\omega\varepsilon(\bar{x})$, for the inhomogeneous object, and the complex conductivity, $\sigma'_b = \sigma_b - i\omega\varepsilon_b$, for the homogeneous embedding. The scalar Green function is given by

$$g(\bar{x}, \bar{x}') = \frac{\exp(ik_b|\bar{x} - \bar{x}'|}{4\pi|\bar{x} - \bar{x}'|}, \quad k_b = \sqrt{(i\omega\mu_b\sigma'_b)}.$$

In this 3D case the field function u_j^{inc} to be replaced by the incident electric field vector $\bar{E}_j^{\text{inc}}$ and the scattered field data u_j^{sct} has to be replaced by either the measured scattered electric field vector $\bar{E}_j^{\text{sct}}$ for an electric dipole receiver or the measured scattered magnetic field vector $\bar{H}_j^{\text{sct}}$ for a magnetic dipole receiver. The governing integral operators become

$$G_S w_j := \begin{cases} [k_b^2 + \nabla\nabla\bullet]\bar{A}_j^E & \text{for an electric dipole receiver,} \\ \sigma'_b \nabla \times \bar{A}_j^E & \text{for a magnetic dipole receiver,} \end{cases}$$

and

$$G_D w_j := [k_b^2 + \nabla\nabla\bullet]\bar{A}_j^E, \qquad \text{where } \bar{A}_j^E(\bar{x}) = \int_D g(\bar{x}, \bar{x}')\bar{w}_j^E(\bar{x}')dv(\bar{x}').$$

We will illustrate the performance of this type of inversion scheme by presenting some inversion results from 3D electromagnetic experimental data.

4. Integral Operators for Electric and Magnetic Contrast

Secondly, we consider the 3D electromagnetic inversion problem. where the scattering object has both electric contrast χ^E and magnetic contrast χ^H with respect to its embedding. In addition the electric contrast sources, we also deal with the magnetic contrast sources

$$\bar{w}_j^H(\bar{x}) = \chi^H(\bar{x})\bar{H}(\bar{x}), \quad \text{where} \quad \chi^H(\bar{x}) = \frac{\mu(\bar{x})}{\mu_b} - 1,$$

with permeability, $\mu(\bar{x})$, for the inhomogeneous object, and permeability, μ_b, for the homogeneous embedding. In this 3D case the cost functional has to be extended to the following form

$$\begin{aligned} F_n \;=\; & [F_S^E(\bar{w}_j^E, \bar{w}_j^H) + F_{D,n}^E(\bar{w}_j^E, \bar{w}_j^H, \chi^E)]\frac{1}{V}\int_D \frac{|\nabla\chi^E|^2 + (\delta_n^E)^2}{|\nabla\chi_{n-1}^E|^2 + (\delta_n^E)^2}dv \\ & + [F_S^H(\bar{w}_j^E, \bar{w}_j^H) + F_{D,n}^H(\bar{w}_j^E, \bar{w}_j^H, \chi^H)]\frac{1}{V}\int_D \frac{|\nabla\chi^H|^2 + (\delta_n^H)^2}{|\nabla\chi_{n-1}^H|^2 + (\delta_n^H)^2}dv \end{aligned}$$

where

$$F_S^E(\bar{w}_j^E, \bar{w}_j^H) = \frac{\sum_j \|\bar{E}_j^{\text{sct}} - G_S^E(\bar{w}_j^E, \bar{w}_j^H)\|_S^2}{\sum_j \|\bar{E}_j^{\text{sct}}\|_S^2} \quad \text{for an electric dipole receiver,}$$

$$F_S^H(\bar{w}_j^E, \bar{w}_j^H) = \frac{\sum_j \|\bar{H}_j^{\text{sct}} - G_S^H(\bar{w}_j^E, \bar{w}_j^H)\|_S^2}{\sum_j \|\bar{H}_j^{\text{sct}}\|_S^2} \quad \text{for a magnetic dipole receiver,}$$

and

$$F_{D,n}^E(\bar{w}_j^E, \bar{w}_j^H, \chi^E) = \frac{\sum_j \|\chi^E\bar{E}_j^{\text{inc}} - \bar{w}_j^E + G_D^E(\bar{w}_j^E, \bar{w}_j^H)\|_D^2}{\sum_j \|\chi_{n-1}^E\bar{E}_j^{\text{inc}}\|_D^2},$$

$$F_{D,n}^H(\bar{w}_j^E, \bar{w}_j^H, \chi^H) = \frac{\sum_j \|\chi^H\bar{H}_j^{\text{inc}} - \bar{w}_j^H + G_D^H(\bar{w}_j^E, \bar{w}_j^H)\|_D^2}{\sum_j \|\chi_{n-1}^H\bar{H}_j^{\text{inc}}\|_D^2},$$

The governing integral operators become

$$G_S^E(\bar{w}_j^E, \bar{w}_j^H) = [k_b^2 + \nabla\nabla\bullet]\bar{A}^E + i\omega\mu_b \nabla \times \bar{A}^H, \quad G_S^H(\bar{w}_j^E, \bar{w}_j^H) = \sigma_b' \nabla \times \bar{A}^E + [k_b^2 + \nabla\nabla\bullet]\bar{A}^H,$$

for observation points in the data domain S,

and

$$G_D^E(\bar{w}_j^E, \bar{w}_j^H) = [k_b^2 + \nabla\nabla\bullet]\bar{A}^E + i\omega\mu_b \nabla \times \bar{A}^H, \quad G_D^H(\bar{w}_j^E, \bar{w}_j^H) = \sigma_b' \nabla \times \bar{A}^E + [k_b^2 + \nabla\nabla\bullet]\bar{A}^H,$$

for observation points in the data domain D,

where

$$\bar{A}^E(\bar{x}) = \int_D g(\bar{x}, \bar{x}')\bar{w}_j^E(\bar{x}')dv(\bar{x}') \quad \text{and} \quad \bar{A}^H(\bar{x}) = \int_D g(\bar{x}, \bar{x}')\bar{w}_j^H(\bar{x}')dv(\bar{x}')$$

The minimization of the extended cost functional is carried out iteratively in three alternate steps:

- For given electric contrast χ_{n-1}^E and magnetic contrast χ_{n-1}^H, the contrast source vector $\{\bar{w}_j^E, \bar{w}_j^H\}$ is updated via conjugate gradient directions of the cost functional.
- For given electric contrast sources $\bar{w}_{j,n}^E$ and magnetic contrast sources $\bar{w}_{j,n}^H$, the electric contrast χ^E is updated via preconditioned conjugate directions.
- For given electric contrast sources $\bar{w}_{j,n}^E$ and magnetic contrast sources $\bar{w}_{j,n}^H$, the magnetic contrast χ^H is updated via preconditioned conjugate directions.

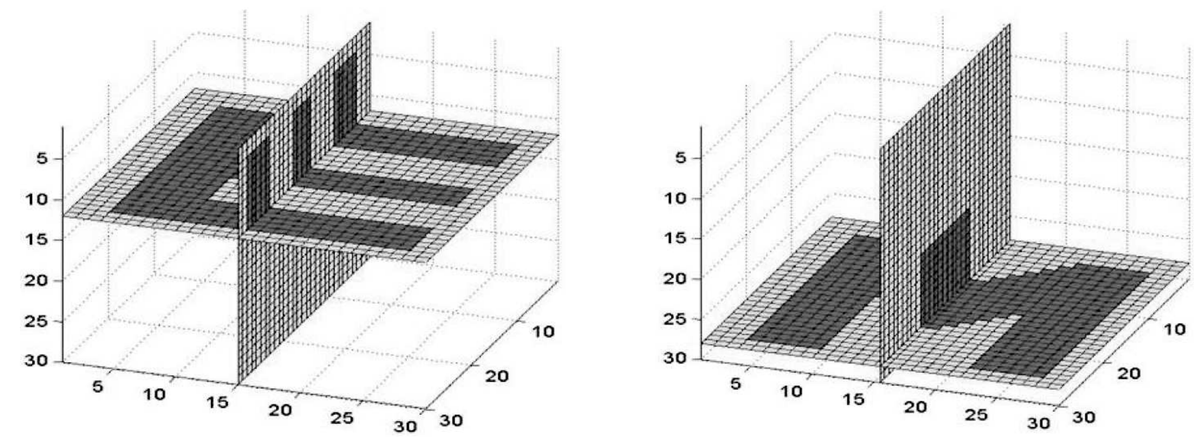

Figure 1: 3D scattering object in a $3\lambda \times 3\lambda \times 3\lambda$ vacuum domain with disjoint electric and magnetic contrast.

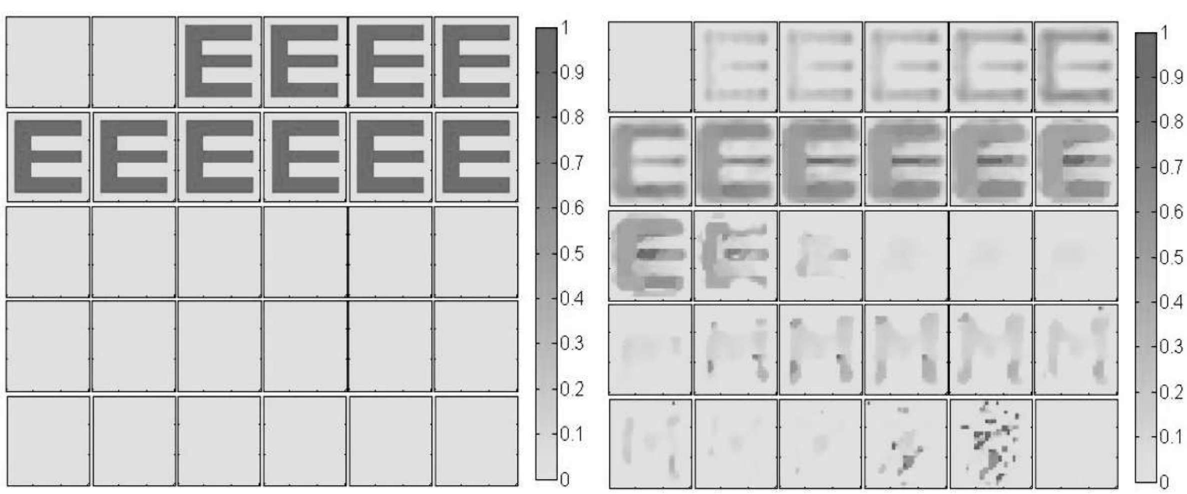

Figure 2: Exact (left) and reconstructed (right) of the real part of the electric contrast, at 30 different horizontal planes.

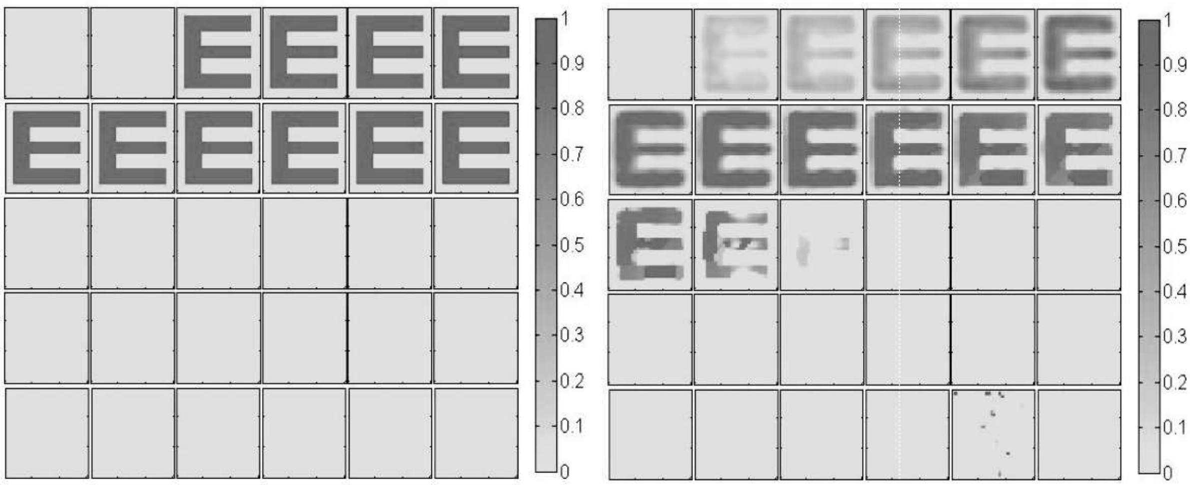

Figure 3: Exact (left) and reconstructed (right) of the imaginary part of the electric contrast, at 30 different horizontal planes.

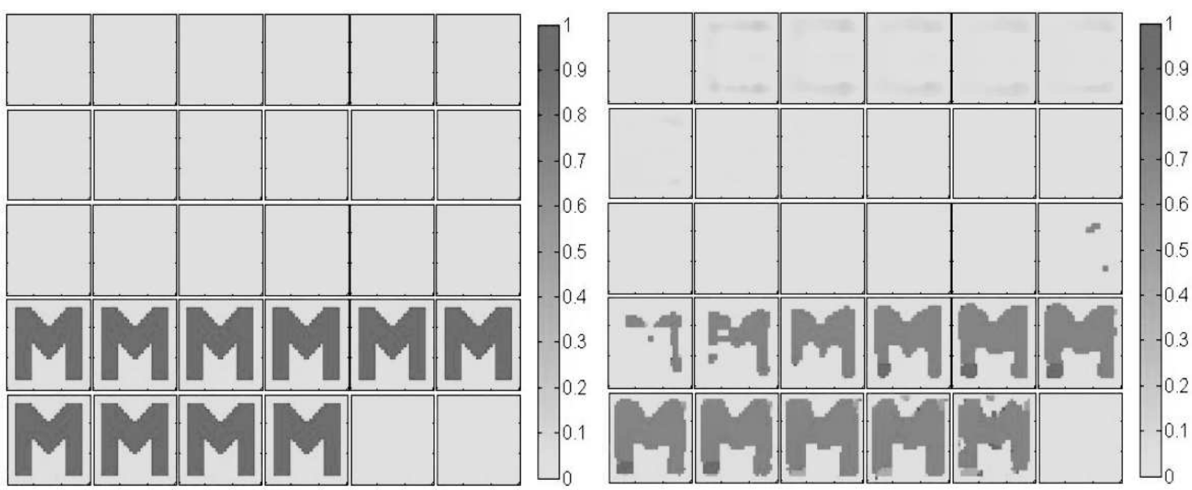

Figure 4: Exact (left) and reconstructed (right) magnetic contrast, at 30 different horizontal planes.

As numerical example we have simulated electromagnetic field data from an object in a vacuum domain with size of $3\lambda \times 3\lambda \times 3\lambda$. One part of the object is "E"-shaped and has only electric contrast given by the complex contrast function $\chi^E = 1 + 1i$, while the other part is "M"-shaped and has only magnetic contrast given by the real contrast function $\chi^H = 1$ (see Figure 1). We use vertical magnetic dipoles both as transmitters and as receivers. In an area above the domain under investigation, 30 transmitters have been located, viz., at the vertical position $x_3 = -0.1\lambda$ In an area below the domain under investigation, 30 receivers have been located, viz., at the vertical position $x_3 = 3.1\lambda$. Hence, we have only 900 complex-valued data points. The square domain D under investigation is subdivided into $30 \times 30 \times 30$. This means that we have 27000 unknown complex-valued electric contrast points plus 27000 unknown real-valued magnetic contrast points. The reconstruction results are given in Figures 2–4. Although the number of unknowns is much larger than the number of known data points, we observe a very good reconstruction in the horizontal plane through the middle of the "E"-shaped object (see Figure 3) and the middle of the "M"-shaped object (see Figure 4), while the reconstruction deteriorates towards the top and bottom part the objects.

We conclude that the present extended form of the MR-CSI method enables the full nonlinear 3D inversion of large scale electromagnetic data.

REFERENCES

1. Abubakar and P. M. van den Berg, "Iterative forward and inverse algorithms based on domain integral equations for three-dimensional electric and magnetic objects," *Journal of Computational Physics*, Vol. 195, 236–262, 2004.